Parallel and Coupled Perpendicular Transitions of RbCs 640 nm System: Mass-Resolved Resonance Enhanced Two-Photon Ionization in a Cold Molecular Beam

Yonghoon Lee,[†] Youngjee Yoon,[‡,§] Sungyul Lee,[⊥] Jin-Tae Kim,[¶] and Bongsoo Kim*[,‡]

Advanced Photonics Research Institute, Gwangju Institute of Science and Technology, Gwangju 500-712, Korea, College of Environmental Science and Applied Chemistry (BK21), Kyunghee University, Kyungki-do 449-701, Korea, Department of Photonic Engineering, Chosun University, Gwangju 501-759, Korea, and Department of Chemistry, KAIST, Daejeon 305-701, Korea

Received: April 17, 2008; Revised Manuscript Received: May 16, 2008

We have investigated the RbCs 640 nm system by mass-resolved resonance enhanced two-photon ionization in a cold molecular beam. Very complex vibronic structures were observed between 15420 and 15990 cm^{-1}. The parallel transitions of 2 $^3\Pi_0$ $v' = 4-20 \leftarrow$ X $^1\Sigma^+$ $v'' = 0$ were identified by rotationally resolved spectra. Molecular constants and a Rydberg−Klein−Rees potential energy curve of the 2 $^3\Pi_0$ state were determined. The regular vibrational spacing of the parallel transition indicated that the 2 $^3\Pi_0$ state is not significantly perturbed by nearby excited electronic states. The complexity of the observed vibronic structures has been attributed to the coupled perpendicular transitions of 2 $^1\Pi$, 2 $^3\Pi_1$, and 3 $^3\Sigma_1^+ \leftarrow$ X $^1\Sigma^+$ $v'' = 0$. For the perpendicular bands observed in the lower-energy spectral region between 15420 and 15630 cm^{-1} where the onsets of the 2 $^3\Pi_1$ and 3 $^3\Sigma_1^+ \leftarrow$ X $^1\Sigma^+$ transitions are located, the upper electronic states and the vibrational quantum numbers were assigned. Perturbations of 2 $^3\Pi_1-3$ $^3\Sigma_1^+$ and 2 $^1\Pi-3$ $^3\Sigma_1^+$ have been identified by the observed level shifts.

1. Introduction

Alkali metal diatomic molecules have been broadly investigated, both experimentally and theoretically and have attracted much attention from various fields in chemistry and physics, for example, in molecular spectroscopy, photodissociation dynamics, control of chemical reactions, and photoassociation spectroscopy. Recent rapid progress in experiments with ultracold molecules has mainly focused on the alkali metal diatomic molecules. The potential application of ultracold polar molecules such as heteronuclear alkali metal diatomic molecules to qubits for quantum computation was proposed by DeMille.[1] Owing to the technical convenience of atomic cooling, RbCs has been suggested as one of the promising candidates for qubit generation among polar molecules.[1] Consequently, there is an increasing need for accurate spectroscopic information on the alkali metal diatomic molecules, for example, on the potential energy curves of ground and excited electronic states and interactions among different electronic states.

RbCs is one of the heavy heteronuclear alkali metal diatomic molecules. After early observations of the absorption bands of RbCs by Walter and Barratt,[2] Loomis and Kusch,[3] and Kusch,[4] high-resolution spectroscopic investigations have been performed. For the ground X $^1\Sigma^+$ state, molecular constants and potential energy curves have been experimentally determined.[5–8] For the excited electronic states, the 3 $^1\Sigma^+$, 7 $^1\Sigma^+$, 2 $^1\Pi$, 4 $^1\Pi$, and 5 $^1\Pi$ states were identified by laser-induced fluorescence (LIF) and Fourier transform (FT) spectroscopy[9] and the 4 $^1\Sigma^+$, 5 $^1\Sigma^+$, 3 $^1\Pi$, and 1 $^3\Delta$ states were identified by mass-resolved resonance enhanced two-photon ionization (RE2PI) in cold molecular beams.[10–12] The complexity of the vibronic structures of heavy heteronuclear alkali metal diatomic molecules is induced by the lack of inversion symmetry (g and u), very congested energy levels, and strong spin−orbit interactions. The nearby excited electronic states with the same Ω ($= \Lambda + \Sigma$ where Λ and Σ are the projections of total electronic orbital angular momentum and total electron spin on the internuclear axis, respectively) symmetry can be strongly coupled through the spin−orbit interactions under these circumstances. Recently, deperturbations of the low-lying strongly coupled systems of RbCs 2 $^1\Sigma^+-1$ $^3\Pi$ and 1 $^1\Pi-2$ $^3\Sigma^+-1$ $^3\Pi$ through spin−orbit interactions have been reported.[13,14] The latter system was employed for producing ultracold X $^1\Sigma^+$ RbCs molecules.[14]

The first theoretical investigation of RbCs was reported by Pavolini et al.[15] Allouche et al. calculated nonrelativistic potential energy curves of the 30 lowest electronic $\Lambda\Sigma$ states of RbCs in Hund's case (a) and compared their theoretical predictions with experimental results.[16] This calculation is in very good agreement with experimental values within 1−2% of the electronic term value and the equilibrium internuclear distance although the spin−orbit interactions were not included. Subsequently, Fahs et al. provided calculations including spin−orbit interactions of RbCs.[17] Recently, Lim et al. have reported potential energy curves for the 28 lowest $\Lambda\Sigma$ states and also 49 Ω states resulting from spin−orbit coupling between the $\Lambda\Sigma$ states, and the effects of the spin−orbit interaction on the dipole moment.[18]

In this work, we report a newly identified parallel transition of 2 $^3\Pi_0 \leftarrow$ X $^1\Sigma^+$ and coupled perpendicular transitions of 2 $^1\Pi$, 2 $^3\Pi_1$, and 3 $^3\Sigma_1^+ \leftarrow$ X $^1\Sigma^+$ observed by mass-resolved RE2PI in a cold molecular beam. Very complex vibronic structures have been observed in our RE2PI spectrum near 640 nm. The 2 $^3\Pi_0$ state, however, showed a very regular vibronic

* To whom correspondence should be addressed. E-mail: bongsoo@kaist.ac.kr. Fax: +82-42-869-2810.
† Advanced Photonics Research Institute.
‡ KAIST.
§ Current Address: Memory Division, Samsung Electronics Co., LTD., Banwol-dong, Hwasung-City, Gyeonggi-do 445-701, Korea.
⊥ Kyunghee University.
¶ Chosun University.

10.1021/jp803360w CCC: $40.75
Published on Web 07/17/2008

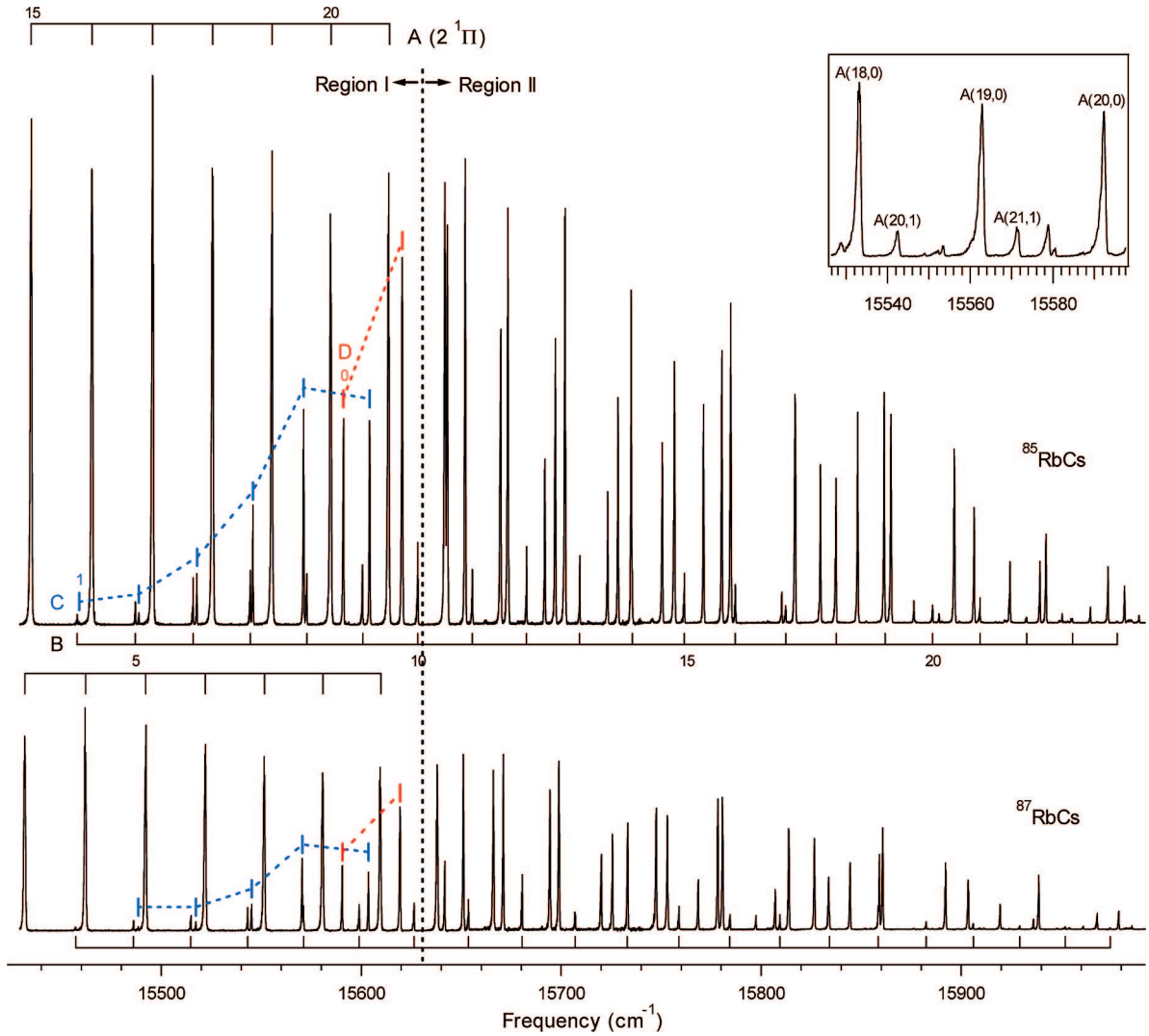

Figure 1. Low-resolution RE2PI spectra of (top) ^{85}RbCs and (bottom) ^{87}RbCs between 15420 and 15990 cm^{-1} obtained by expanding Ar carrier gas at 760 Torr. A, B, C, and D progressions and their vibrational quantum numbers are indicated. The inset shows the low-resolution RE2PI spectrum of ^{85}RbCs between 15528 and 15598 cm^{-1} obtained by expanding Ar carrier gas at 560 Torr. Upper and lower vibrational quantum numbers (v', v'') of the A bands are indicated.

structure, indicating the absence of significant perturbation. By fitting the observed term values of these parallel bands, we have determined the molecular constants and the Rydberg−Klein−Rees (RKR) potential energy curve of the 2 $^3\Pi_0$ state. The origin of the complex vibronic structures has been attributed to strong spin−orbit interactions among the $\Omega = 1$ states. In the lower energy spectral region where the onsets of the 2 $^3\Pi_1$ and 3 $^3\Sigma_1^+$ ← X $^1\Sigma^+$ transitions were observed, we have identified the electronic symmetry and the vibrational quantum numbers of the upper vibronic states for the observed perpendicular bands. The diagonal spin−orbit interaction constant of the 2 $^3\Pi$ state has been estimated from the observed splitting of the electronic term values of the $\Omega = 0$ and 1 components.

2. Experiment

Our experimental apparatus and techniques have been previously discussed.[19] Briefly, we prepared RbCs by expanding Rb and Cs vapor with Kr or Ar gas through a high-temperature pulsed nozzle. In this experiment, the temperature of the nozzle was maintained at 290 °C. The nozzle diameter was 800 μm. The pulsed jet was collimated by a 1.2 mm diameter skimmer located 7 cm from the nozzle. $RbCs^+$ ions were generated by the absorption of two photons from a dye laser (Lambda Physik Scanmate 2E) pumped by the second harmonic of a Nd:YAG laser (Spectra Physics GCR-150). The isotopomers of RbCs (^{85}Rb^{133}Cs and ^{87}Rb^{133}Cs) were separated and detected by a linear time-of-flight (TOF) mass spectrometer ($m/\Delta m \approx 500$). Low-resolution RE2PI spectra were obtained with 0.12 cm^{-1} laser line width. When rotationally resolved RE2PI spectra were recorded, we installed an intracavity étalon which narrows the laser line width to 0.02 cm^{-1}. The wavelength of the dye laser was calibrated by a wavemeter (Burleigh WA-4500) and Ne optogalvanic spectra for the low-resolution scans. For the wavelength calibration of the high-resolution scans, I_2 LIF spectra were obtained simultaneously.[20]

3. Results and discussion

3.1. Overview of the RbCs 640 nm System. Figure 1 shows the low-resolution RE2PI spectra of ^{85}RbCs and ^{87}RbCs isotopomers between 15420 and 15990 cm^{-1} obtained by coexpanding Ar carrier gas at 760 Torr. The observed RE2PI spectra show very complex and rich vibronic structures, particularly above 15630 cm^{-1} (compare regions I and II indicated in Figure 1). We identified four vibrational progres-

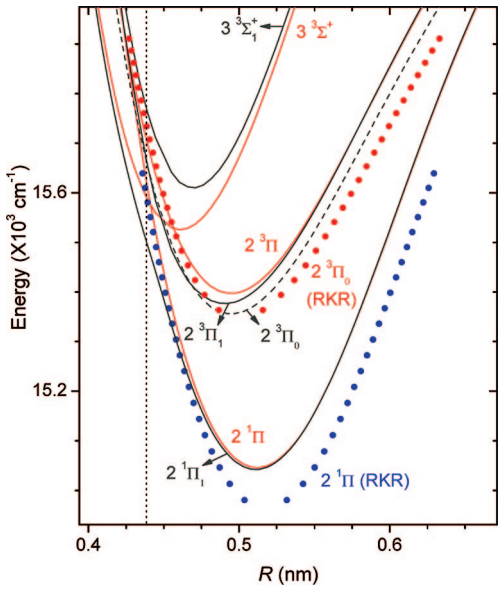

Figure 2. Ab initio potential energy curves of RbCs for the 2 $^1\Pi$, 2 $^3\Pi$, and 3 $^3\Sigma^+$ states from ref 16 (red solid lines) and those of the corresponding Ω states from ref 17 (dark gray lines). The solid and dashed dark gray lines represent the Ω = 1 (2 $^1\Pi$, 2 $^3\Pi_1$, and 3 $^3\Sigma_1^+$) and 0 (2 $^3\Pi_0$) states, respectively. For the 2 $^1\Pi$ (blue filled circles) and 2 $^3\Pi_0$ (red filled circles) states, the RKR potential energy curves from ref 9 and this work, respectively, are shown together. The vertical dotted line represents the Franck−Condon region (R_e of the X $^1\Sigma^+$ state, 4.379 Å from ref 16). The origin of the ordinate axis is set to the potential minimum of the X $^1\Sigma^+$ state.

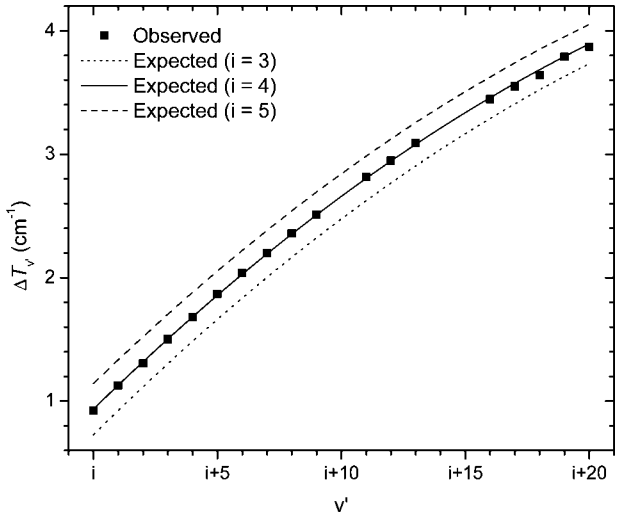

Figure 3. Observed isotope shifts of the B progression between ^{85}RbCs and ^{87}RbCs and expected values with the assignments of i (v' of the B band of ^{85}RbCs at 15458.0 cm^{-1}) to 3, 4, and 5.

sions indicated as A, B, C, and D in Figure 1. The A progression is easily assigned to the 2 $^1\Pi$ v' = 15−21 ← X $^1\Sigma^+$ v'' = 0 transitions by comparing the observed vibronic band positions with those reported by Gustavsson et al.[9] They determined the molecular constants and the RKR potential energy curve of the 2 $^1\Pi$ state up to the v' = 21 level using LIF and FT spectroscopy. The progression of vibronic bands for 2 $^1\Pi$ $v' \geq$ 22 ← X $^1\Sigma^+$ v'' = 0 transitions seems to continue to the higher spectral region above 15630 cm^{-1}. However, the observed vibronic structures in region II became notably more irregular and complex than those in region I, and it was difficult to identify the vibronic bands of 2 $^1\Pi$ $v' \geq$ 22 ← X $^1\Sigma^+$ v'' = 0 from the vibrational spacings, $\Delta G_{v'}$. Unlike other progressions,

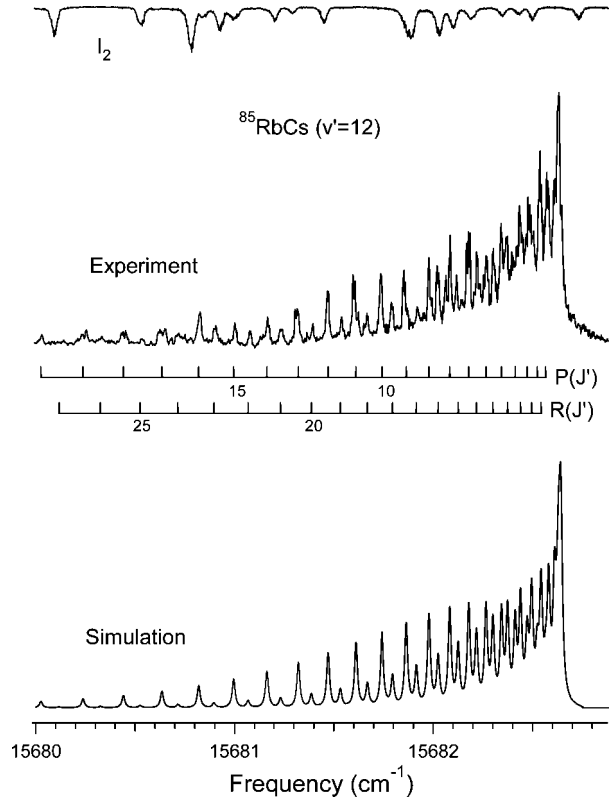

Figure 4. High-resolution RE2PI spectrum of the v' = 12 ← v'' = 0 band of the B progression. The top trace corresponds to the LIF spectrum of I_2, the middle trace to the RE2PI spectrum of ^{85}RbCs, and the bottom trace to the simulation generated from the band constants. The molecular beam was expanded with 360 Torr of Ar. In the simulation, we set the laser line width to 0.018 cm^{-1}, T_{rot} = 2.5 K, and included only P and R branches.

the B progression had very regular vibrational spacing in the whole spectral region we observed. The onsets of the C and D progressions are located in region I. The extension of the progressions C and D, as well as A, to region II could not be confidently identified owing to irregular and complex vibronic structures.

To confirm the initial state of the observed vibronic transitions we changed the expansion condition to 560 Torr of Ar and obtained the low-resolution RE2PI spectrum of ^{85}RbCs at a higher vibrational temperature (see the inset in Figure 1). The vibrationally hot bands, 2 $^1\Pi$ v' = 20 and 21 ← X $^1\Sigma^+$ v'' = 1 indicated in the inset of Figure 1 confirm that the initial state of the observed vibronic transitions is X $^1\Sigma^+$ v'' = 0. The observed differences in the vibronic band positions from v'' = 0 and 1 (49.80 and 49.75 cm^{-1} for v' = 20 and 21, respectively) are consistent with the energy difference between the v'' = 0 and v'' = 1 levels of the ground electronic state. (49.7921 cm^{-1}).[8]

Figure 2 shows the ab initio potential energy curves of RbCs for the 2 $^1\Pi$, 2 $^3\Pi$, and 3 $^3\Sigma^+$ states reported by Allouche et al.[16] and those for the corresponding Ω states reported by Fahs et al.[17] The RKR potential energy curves of the 2 $^1\Pi$ (from ref 9) and 2 $^3\Pi_0$ (from this work) states (see the following section for the construction of the RKR potential energy curve of the 2 $^3\Pi_0$ state) are compared with the ab initio potential curves in Figure 2. The vertical dotted line represents the Franck−Condon region where RbCs in the X $^1\Sigma^+$ v'' = 0 level can be excited by vertical transitions. As shown in Figure 2, the ab initio calculation predicts that the 2 $^1\Pi$, 2 $^3\Pi$, and 3 $^3\Sigma^+$ states can be observed between 15420 and 15990 cm^{-1}.[16] Allowing

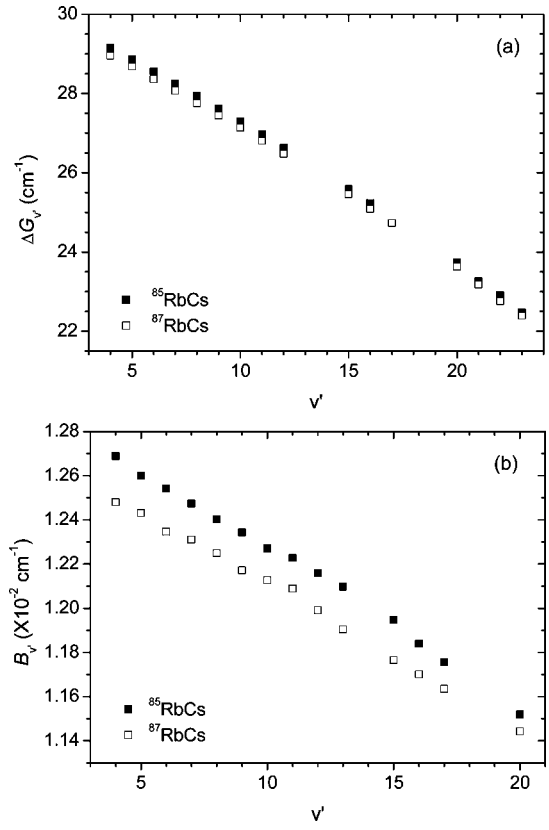

Figure 5. Plots of (a) $\Delta G_{v'}$ and (b) $B_{v'}$ versus v' for the B progression.

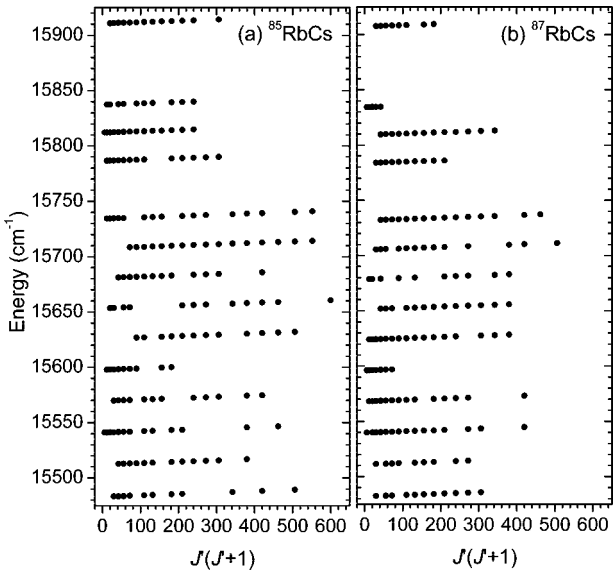

Figure 6. Data range of the term values of the B progression for a Dunham fit.

spin−orbit interactions among the ΛΣ states, we find that one parallel transition, 2 $^3\Pi_0 \leftarrow$ X $^1\Sigma^+$, and three perpendicular transitions, 2 $^1\Pi$, 2 $^3\Pi_1$, and 3 $^3\Sigma_1^+ \leftarrow$ X $^1\Sigma^+$, may contribute to the observed vibronic structures in the RE2PI spectrum of Figure 1. From these, the B progression that shows regular vibrational spacings can be assigned to the parallel 2 $^3\Pi_0 \leftarrow$ X $^1\Sigma^+$ transition and the observed complexity in the vibronic structures can be attributed to the strong spin−orbit interactions ($\Delta\Omega = 0$) among the $\Omega = 1$ states. Consequently, the candidates for the final electronic states of the C and D progressions are the 2 $^3\Pi_1$ and 3 $^3\Sigma_1^+$ states.

TABLE 1: Dunham Coefficients of the 2 $^3\Pi_0$ State of ^{85}RbCs. All Values Are in cm^{-1}

l	Y_{l0}	$\sigma(Y_{l0})^a$	Y_{l1}	$\sigma(Y_{l1})^a$
0	−0.00142	0.00042	1.2984×10^{-2}	1.5×10^{-5}
1	30.5175	0.0026	-6.89×10^{-5}	1.2×10^{-6}
2	-1.2883×10^{-1}	2.3×10^{-4}		
3	-1.0518×10^{-3}	6.0×10^{-6}		

[a] Standard deviations of Y_{l0} and Y_{l1}.

TABLE 2: Vibrational Term Values and Turning Points of the 2 $^3\Pi_0$ State of ^{85}RbCs Obtained by an RKR Procedure

v	$G_v + Y_{00}$	R_{min} (Å)	R_{max} (Å)
	$T_e = 15348.2928$ cm^{-1} [a]	$R_e = 5.0051$ Å	
0	15.2235	4.8654	5.1579
1	45.4799	4.7706	5.2791
2	75.4692	4.7086	5.3677
3	105.1851	4.6602	5.4429
4	134.6212	4.6195	5.5106
5	163.7713	4.5841	5.5733
6	192.6290	4.5525	5.6323
7	221.1881	4.5239	5.6887
8	249.4422	4.4975	5.7431
9	277.3850	4.4730	5.7958
10	305.0101	4.4501	5.8472
11	332.3114	4.4284	5.8976
12	359.2825	4.4079	5.9472
13	385.9170	4.3883	5.9962
14	412.2086	4.3696	6.0446
15	438.1511	4.3516	6.0927
16	463.7382	4.3342	6.1405
17	488.9634	4.3173	6.1881
18	513.8206	4.3009	6.2357
19	538.3034	4.2849	6.2832
20	562.4055	4.2693	6.3309

[a] Y_{00} is corrected.

3.2. Parallel ($\Delta\Omega = 0$) Bands. We have obtained rotationally resolved spectra of the B bands ($v' = 4-13$, 15−17, and 20 for ^{85}RbCs and ^{87}RbCs). The rotationally resolved spectra of the other B bands could be not obtained successfully because of spectral overlap or weak band intensity. To determine the band constants, we performed band-by-band fits of the observed transition frequencies, ν, using the following standard equation,

$$\nu = \nu_0 + B_{v'}J'(J'+1) - D_{v'}[J'(J'+1)]^2 - \{B_{v''}J''(J''+1) - D_{v''}[J''(J''+1)]^2\} \quad (1)$$

where ν_0 represents the band origin. The rotational and centrifugal distortion constants for the ground state, $B_{v''}$ and $D_{v''}$, were fixed at the values reported by Fellows et al.[8] The upper-state $D_{v'}$ was also fixed at the value calculated from the ab initio potential energy curve of the 2 $^3\Pi$ state.[16] For the rotational analyses and simulations presented in this work, we used the PGOPHER program.[21] The determined band constants are listed in the Supporting Information. Absolute vibrational quantum numbers were determined from the observed isotope shifts, $\Delta T_{v'}$, defined as $T_{v'}(^{85}\text{RbCs}) - T_{v'}(^{87}\text{RbCs})$. Assuming v' of the B band observed at the lowest transition frequency (15457.9 cm^{-1} for ^{85}RbCs) as 3, 4, and 5, the $T_{v'}$ values of ^{85}RbCs and ^{87}RbCs isotopomers were fitted simultaneously by the following simple mass-reduced relation

$$T_{v'} = T_e + \omega_e\rho(v'+1/2) - \omega_e x_e[\rho(v'+1/2)]^2 \quad (2)$$

The electronic term value, harmonic vibrational frequency, and anharmonic vibrational constant are represented by T_e, ω_e, and

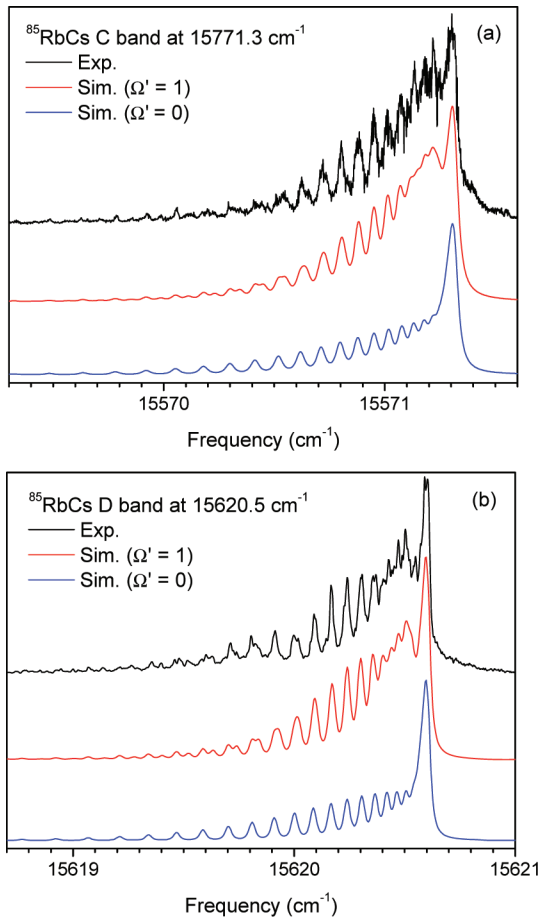

Figure 7. High-resolution spectra of (a) the C band ($v' = 5 \leftarrow v'' = 0$) at 15771.3 cm^{-1} and (b) the D band ($v' = 1 \leftarrow v'' = 0$) at 15620.5 cm^{-1}, and their simulations as perpendicular ($\Omega' = 1$) and parallel ($\Omega' = 0$) bands. The simulations as perpendicular bands were obtained by band contour fits and those as parallel bands generated from the same band constants except for the Ω' values. The spectrum of the D band below 15620 cm^{-1} was slightly congested by a hot band transition. The molecular beam was expanded with 760 Torr of Ar.

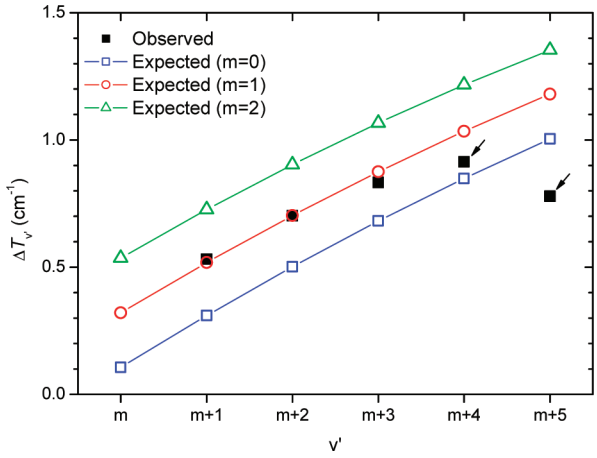

Figure 8. Observed isotope shifts of the C progression between ^{85}RbCs and ^{87}RbCs and expected values with the assignments of m (v' of the C band of ^{85}RbCs at 15459.0 cm^{-1}) to 0, 1, and 2. The arrows indicate the observed values which deviate significantly from the expected values due to perturbations between the 2 $^3\Pi_1$ $v' = 5$ and 6 and 3 $^3\Sigma_1^+$ $v' = 0$ levels (see section 3.3).

$\omega_e x_e$, respectively. The constant ρ (= 1 for ^{85}RbCs and 0.992963624 for ^{87}RbCs)[22] is given by $\rho = \sqrt{\mu/\mu_\alpha}$, where μ is the reduced mass of the major isotopomer, ^{85}RbCs, and μ_α represents that of ^{87}RbCs. The expected $\Delta T_{v'}$ values were calculated from the fitted parameters using the following equation:

$$\Delta T_{v'} = T_{v'}(^{85}\text{RbCs}) - T_{v'}(^{87}\text{RbCs}) \quad (3a)$$

$$= \omega_e(v' + 1/2) - \omega_e x(v' + 1/2)^2 - [\omega_e\rho(v' + 1/2) - \omega_e x_e\rho^2(v' + 1/2)^2] \quad (3b)$$

Figure 3 compares the observed $\Delta T_{v'}$ values with the expected values. The observed $\Delta T_{v'}$ values are in very good agreement with the expected values with i (v' of the B band observed at the lowest transition frequency) = 4. The absolute vibrational quantum numbers of the B bands are thus assigned. Figure 4 shows the rotationally resolved spectrum of the B $v' = 12 \leftarrow v'' = 0$ band and the simulation generated from the band constants listed in the Supporting Information. Parallel and perpendicular transitions induced by an electric dipole transition moment are distinguished by rotational branches observed in a vibronic band.[23] Parallel bands ($\Delta\Lambda = 0$ in Hund's case (a) or $\Delta\Omega = 0$ in Hund's case (c)) consist of P ($\Delta J = -1$) and R ($\Delta J = +1$) branches of comparable intensity. Perpendicular bands ($\Delta\Lambda = \pm 1$ in Hund's case (a) or $\Delta\Omega = \pm 1$ in Hund's case (c)) have a strong Q ($\Delta J = 0$) branch of approximately twice the intensity of the P and R branches. As shown in Figure 4, the B band consists of P and R branches and thus becomes a parallel transition. Figure 5 shows (a) the vibrational spacing, $\Delta G_{v'}$, defined as $G_{v'+1} - G_{v'}$, and (b) $B_{v'}$ values of the B progression versus v'. Regular features of the plots of $\Delta G_{v'}$ and $B_{v'}$ vs v' of the B progression indicate that there are no significant perturbations on the upper vibronic levels caused by the nearby levels belonging to other excited electronic states. Among the excited electronic states located in the observed spectral region, the only excited electronic state accessible through a parallel transition from the X $^1\Sigma^+$ $v'' = 0$ level is the 2 $^3\Pi_0$ state (see Figure 2). The perturbations between the 2 $^3\Pi_0$ state and the nearby 2 $^1\Pi$, 2 $^3\Pi_1$, and 3 $^3\Sigma_1^+$ states of $\Omega = 1$ through spin−orbit interactions ($\Delta\Omega = 0$) are forbidden. This is consistent with the observed regularity of the band constants of the B progression. The absence of significant perturbations and the rotational structure let the upper electronic state of the B progression be assigned to the 2 $^3\Pi_0$ state.

To determine the molecular constants of the 2 $^3\Pi_0$ state, we performed a global fit of the observed term values of ^{85}RbCs and ^{87}RbCs to the following mass-reduced Dunham expression using the DParFit 3.3 program:[24]

$$T_{vJ} = T_e + \sum_{l=0}\sum_{m=0} Y_{lm}[\rho(v + 1/2)]^l\{\rho^2[J(J+1) - \Lambda^2]\}^m \quad (4)$$

Figure 6 shows the range of the term value data included in our fit (202 term values for ^{85}RbCs and 175 term values for ^{87}RbCs). The observed rotational structure of the B bands, which consists of P and R branches, can be treated as a simple case of $^1\Sigma^+ \leftarrow {}^1\Sigma^+$ transition. Therefore, we performed the fit with $\Lambda = 0$. The Dunham-type zero-point energy correction was conducted using the relation, $Y_{00} = (Y_{01} + Y_{20})/4 - [(Y_{11}Y_{10})/(12Y_{01})] + [(Y_{11}Y_{10})/(12Y_{01})]^2/Y_{01}$.[25] The determined Dunham coefficients of the 2 $^3\Pi_0$ state are listed in Table 1. The data range of our term values is limited to lower J' levels ($\leq$24) because of the extensive rotational cooling in the pulsed molecular beam, and thus the centrifugal distortion constants, Y_{lm}'s ($m \geq 2$), of the 2 $^3\Pi_0$ state could not be determined accurately. Therefore, they were not included in the fit. The

TABLE 3: Theoretically and Experimentally Determined Molecular Constants of the 2 $^1\Pi$, 2 $^3\Pi$, and 3 $^3\Sigma^+$ States and the Corresponding Ω States

		T_e (cm^{-1})	R_e (Å)	ω_e (cm^{-1})	B_e (cm^{-1})
2 $^1\Pi$	theory ($\Sigma\Lambda$)[a]	15046	5.119	33.36	0.01237
	theory ($\Omega = 1$)[b]	15039	5.122	35.2	0.0124
	exptl[c]	14963.622(3)	5.164	32.9255(14)	0.01215169(51)
2 $^3\Pi$	theory ($\Sigma\Lambda$)[a]	15398	4.953	32.13	0.0132
	theory ($\Omega = 1$)[b]	15375	4.894	31.1	0.0135
	theory ($\Omega = 0^+$)[b]	15359	4.942	29.8	0.0133
3 $^3\Sigma^+$	theory ($\Sigma\Lambda$)[a]	15526	4.609	38.98	0.01526
	theory ($\Omega = 1$)[b]	15611	4.696	41.8	0.0147
B (2 $^3\Pi_0$)	this work	15348.2928(96)	5.005	30.5175(26)	0.012984(15)
C (2 $^3\Pi_1$)	this work	15437.34(14)		31.726(96)	

[a] Reference 16. [b] Reference 17. [c] Reference 9.

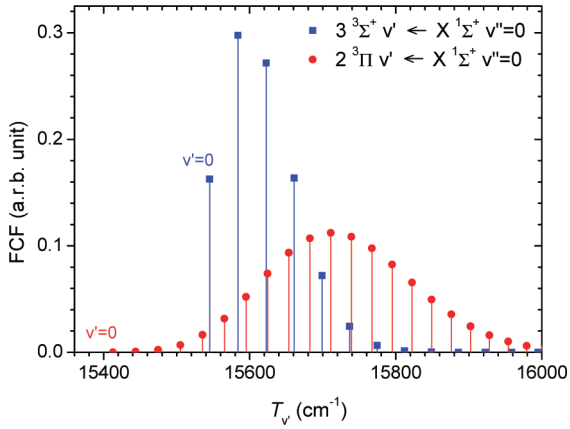

Figure 9. Franck−Condon factors (FCF) of the 3 $^3\Sigma^+$ and 2 $^3\Pi \leftarrow$ X $^1\Sigma^+$ $v'' = 0$ transitions calculated using the ab initio potential energy curves from ref 16.

RKR potential energy curve was constructed using an RKR1 2.0 program[26] with the determined Y_{l0} and Y_{l1} coefficients. The vibrational term values and turning points for the RKR potential energy curve are listed in Table 2. The constructed RKR potential energy curve of the 2 $^3\Pi_0$ state is compared with ab initio potential energy curves in Figure 2.

3.3. Perpendicular (ΔΩ = 1) Bands. The remaining vibronic bands that do not belong to the A and B progressions in the observed RE2PI spectrum can be tentatively attributed to the perpendicular transitions of 2 $^1\Pi$ ($v' \geq 22$), 2 $^3\Pi_1$, and 3 $^3\Sigma_1^+ \leftarrow$ X $^1\Sigma^+$ $v'' = 0$. In region I, the 2 $^1\Pi$ $v' = 15-21$ and 2 $^3\Pi_0$ $v' = 4-10 \leftarrow$ X $^1\Sigma^+$ $v'' = 0$ transitions have been assigned and the onsets of C and D progressions were observed (see Figure 1). The upper electronic states of the C and D progressions can be assigned to the 2 $^3\Pi_1$ and 3 $^3\Sigma_1^+$ states, respectively, from the following observations: (i) Rotational structures of the C and D bands consist of *P*, *Q*, and *R* branches. (ii) The onset of the D progression is located at the higher energy than that of C progression. (iii) The D progression starts suddenly with a considerably strong intensity.

We performed rotational band contour fits for the C and D bands in order to find the Ω values of their final electronic states. Figure 7 compares the high-resolution spectra of the C and D bands at 15771.3 and 15620.5 cm^{-1}, respectively, with their simulations generated assuming that they are perpendicular (*P*, *Q*, and *R* branches) and parallel (P and R branches) bands. The simulations of the C and D bands as perpendicular bands fit the experimental spectra better than those assuming parallel bands. This confirms the Ω = 1 symmetry of the upper electronic states of the C and D bands. The fitted band constants are listed in the Supporting Information.

From the isotope shifts of the C bands, the absolute vibrational quantum numbers of the upper levels were assigned as indicated in Figure 1. Figure 8 compares the observed and expected $\Delta T_{v'}$ values of the C progression. The expected $\Delta T_{v'}$ values were calculated using the same procedure as applied to the B bands (see section 3.2). The $\Delta T_{v'}$ values denoted by the arrows in Figure 8 show a large deviation from the expected values. This indicates curve crossing or strong perturbation for these vibronic levels and thus we excluded these values from the fit. The assignment of m (v' of the C band of ^{85}RbCs observed at the lowest transition frequency, 15459.0 cm^{-1}) to 1 provided the best fit of the observed $\Delta T_{v'}$ values, and those of the higher-lying C bands were successively assigned. The molecular constants (T_e = 15437.34(14) cm^{-1}, ω_e = 31.726(96) cm^{-1}, and $\omega_e x_e$ = 0.457(15) cm^{-1}) and the spin−orbit splitting, which can be regarded as the diagonal spin−orbit coupling matrix element of the 2 $^3\Pi$ state (T_e of 2 $^3\Pi_1$ − T_e of 2 $^3\Pi_0$ = 89 cm^{-1}), were obtained. In Table 3, the experimentally determined molecular constants are compared with the ab initio values of the 2 $^1\Pi$, 2 $^3\Pi$, and 3 $^3\Sigma^+$ states. The procedure comparing the observed and expected $\Delta T_{v'}$ values could not be applied to assign the vibrational quantum numbers of the D bands, since the number of available $\Delta T_{v'}$ values was limited and the D bands were strongly perturbed by the nearby A and C bands. Prior to discussion on the perturbations among the A, C, and D bands, we assigned the vibrational quantum numbers of the D bands at 15591.1 and 15620.5 cm^{-1} to 0 and 1, respectively, through their observed vibronic-band intensity distribution. The vibronic-band intensity distribution of the D progression was strikingly different from those of other progressions. The D progression starts with considerably strong vibronic-band intensity at 15591.1 cm^{-1}. There are no vibronic bands below 15591.1 cm^{-1} which seem to belong to the D progression. Therefore, we assign the D band at 15591.1 cm^{-1} to the 3 $^3\Sigma^+_1$ $v' = 0 \leftarrow$ X $^1\Sigma^+$ $v'' = 0$ transition. This assignment is also supported by the ab initio calculation.[16] If the equilibrium internuclear distance, R_e, of the upper electronic state is close to that of the lower level (X $^1\Sigma^+$ $v'' = 0$, as in the case of our molecular beam experiment), the $v' = 0 \leftarrow v'' = 0$ transition tends to have maximum vibronic-band intensity. The observed vibronic-band intensity distribution of the D progression indicates that R_e of the upper electronic state is close to that of the X $^1\Sigma^+$ state. Among the R_e values of the 2 $^1\Pi$ (5.119 Å), 2 $^3\Pi$ (4.953 Å), and 3 $^3\Sigma^+$ (4.609 Å) states predicted by the ab initio calculation, the R_e value of the 3 $^3\Sigma^+$ state is closest to that of the X $^1\Sigma^+$ state (4.379 Å).[16] Figure 9 shows the Franck−Condon factors of the 2 $^3\Pi$ and 3 $^3\Sigma^+ \leftarrow$ X $^1\Sigma^+$ $v'' = 0$ transitions calculated using the corresponding ab initio potential energy curves and the LEVEL 7.7 program, which closely reproduce the observed vibronic-band intensity

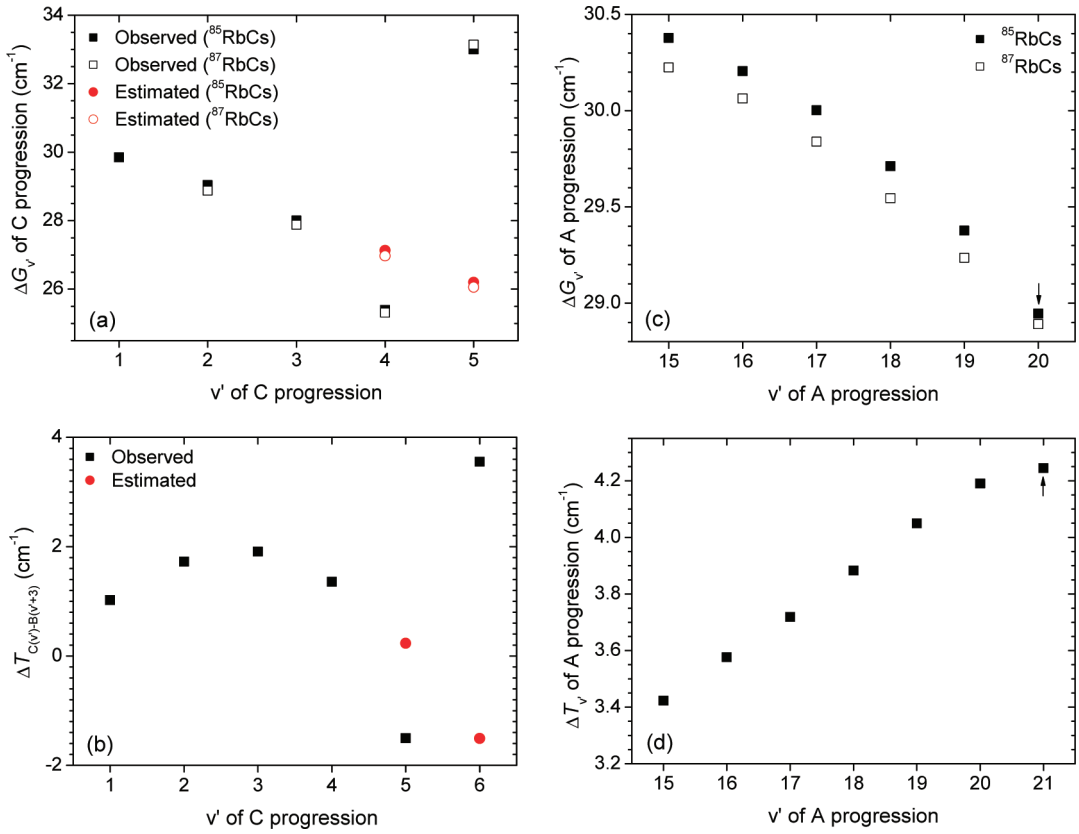

Figure 10. Plots of (a) $\Delta G_{v'}$ of the C progression, (b) $\Delta T_{C(v')\text{-}B(v'+3)}$ versus v' of the C progression, and (c) $\Delta G_{v'}$ and (d) $\Delta T_{v'}$ values of the A progression versus v' of the A progression. The $\Delta G_{v'=4,5}$ values of the C progression and the differences between $T_{v'=5,6}$ of the C progression and the nearest term values of the B progression were calculated using the estimated $T_{v'=5,6}^{depert}$ values (red circles in panels a and b) and compared with the observed values. The arrows in panels c and d indicate the irregular behavior of the $\Delta G_{v'=20}$ (^{85}RbCs) and $\Delta T_{v'=21}$ values of A progression.

distributions of the C and D progression.[16,27] The recent theoretical works predicted that T_e of the 3 $^3\Sigma^+$ state would be located 100−200 cm^{-1} higher than that of the 2 $^3\Pi$ state,[16,18] and the energy difference becomes 20−40 cm^{-1} larger upon the introduction of spin−orbit coupling between the excited states.[17,18] This leads to the assignment of the upper electronic states of the C (lower-lying perpendicular transition) and D (higher-lying perpendicular transition) progressions to the 2 $^3\Pi_1$ and 3 $^3\Sigma_1^+$ states, respectively. From the assignments of the vibrational quantum numbers of the C and D bands, the difference between T_e of the 3 $^3\Sigma_1^+$ state and T_e of the 2 $^3\Pi_1$ state is roughly estimated as ∼160 cm^{-1} with the uncertainty of about 10 cm^{-1}, which comes from the level shifts induced by the perturbations, as discussed in the following paragraph.

As discussed above, the deviation of the C band positions of $v' = 5$ and 6 ← $v'' = 0$ from normal behavior suggests the existence of a perturbation between the 2 $^3\Pi_1$ and 3 $^3\Sigma_1^+$ states. Also, the $\Delta G_{v'}$ and $\Delta T_{v'}$ values of the A progression suggest a perturbation between the 2 $^1\Pi$ and 3 $^3\Sigma_1^+$ states. Figure 10 shows (a) $\Delta G_{v'}$ of the C progression and (b) $\Delta T_{C(v')\text{-}B(v'+3)}$, defined as the difference in vibrational term values between the C band and the nearest B band, versus v' of the C progression, and (c) $\Delta G_{v'}$ and (d) $\Delta T_{v'}$ values of the A progression versus v' of the A progression. The difference in vibrational term values between the C band and the nearest B band corresponds to the spacing between the nearby vibronic levels of the $\Omega = 1$ and 0 components of the 2 $^3\Pi$ state. The vibrational quantum number of the B band nearest to a given C band is larger than that of the C band by as many as 3. Figure 10a clearly shows the irregular behavior of the $\Delta G_{v'}$ values of the C progression. The location of the perturbing 3 $^3\Sigma_1^+$ $v' = 0$ level between the 2 $^3\Pi_1$ $v' = 5$ and 6 levels clearly explains the observed shifts of the 2 $^3\Pi_1$ $v' = 5$ and 6 levels. This location of the 3 $^3\Sigma_1^+$ $v' = 0$ level can shift the 2 $^3\Pi_1$ $v' = 5$ and 6 levels in the opposite direction, red and blue, respectively, with the consequence that the $\Delta G_{v'=4} = G_{v'=5} - G_{v'=4}$ value decreases and the $\Delta G_{v'=5} = G_{v'=6} - G_{v'=5}$ value increases. The deperturbed $T_{v'=5,6}$ values of the 2 $^3\Pi_1$ state could be approximately estimated from the molecular constants determined by fitting the $T_{v'=1-4}$ values. The 2 $^3\Pi_1$ $v' = 5$ and 6 levels of ^{85}RbCs (^{87}RbCs) were found to be shifted by $T_{v'=5}^{obs} - T_{v'=5}^{depert} = 15596.22 - 15597.96 = -1.74$ cm^{-1} (15595.31 − 15596.97 = −1.66 cm^{-1}) and $T_{v'=6}^{obs} - T_{v'=6}^{depert} = 15629.22 - 15624.16 = +5.06$ cm^{-1} (15628.44 − 15623.02 = +5.42 cm^{-1}), respectively. In Figure 10a,b, the $\Delta G_{v'=4,5}$ and $T_{v'=5,6}$ (C) − $T_{v'=8,9}$ (B) values calculated from the estimated $T_{v'=5,6}^{depert}$ values (red circles) of the 2 $^3\Pi_1$ state are shown together. This indicates that the upper level of the D bands selectively perturbs the $\Omega = 1$ component of the 2 $^3\Pi$ state. As shown in Figure 10c,d, the vibronic structure of the 2 $^1\Pi$ $v' = 15-21$ levels is fairly regular. Note that the 2 $^1\Pi$ $v' = 21$ level of ^{85}RbCs is slightly red-shifted from the $\Delta G_{v'=20}$ and $\Delta T_{v'=21}$ values (see the indicated values by arrows in Figure 10c,d). This might be due to the perturbation from the 3 $^3\Sigma_1^+$ $v' = 1$ level. These observations of the levels shifts of the perpendicular bands near the onset of the 3 $^3\Sigma_1^+$ ← X $^1\Sigma_g^+$ transition indicate that the perturbations among the $\Omega = 1$ states are responsible for the complex vibronic structures observed in region II.

4. Conclusion

We have observed very complex and rich vibronic structures of RbCs between 15420 and 15990 cm^{-1} by RE2PI in a cold

molecular beam. The parallel transition of $2\ ^3\Pi_0 \leftarrow X\ ^1\Sigma^+$ and the coupled perpendicular transitions of $2\ ^1\Pi$, $2\ ^3\Pi_1$, and $3\ ^3\Sigma_1^+ \leftarrow X\ ^1\Sigma^+$ were identified. For the $2\ ^3\Pi_0$ state, determination of the molecular constants by a Dunham fit and construction of the potential energy curve by an RKR procedure were performed. The observed spectral complexity can be attributed to the strong spin−orbit interactions among the $2\ ^1\Pi$, $2\ ^3\Pi_1$, and $3\ ^3\Sigma_1^+$ states. Below 15630 cm^{-1}, we have assigned the upper electronic states and the vibrational quantum numbers of the perpendicular transitions, $2\ ^1\Pi\ v' = 15 - 21$, $2\ ^3\Pi_1\ v' = 1 - 6$, and $3\ ^3\Sigma_1^+\ v' = 0$ and $1 \leftarrow X\ ^1\Sigma^+\ v'' = 0$. Particularly, the perturbations of $2\ ^3\Pi_1 - 3\ ^3\Sigma_1^+$ and $2\ ^1\Pi - 3\ ^3\Sigma_1^+$ could be identified from the observed vibronic energy level shifts. Theoretical predictions of spin−orbit interactions among the excited electronic states for RbCs have not been available yet although they could provide valuable information for understanding the multiply coupled electronic states. Ab initio calculations of the spin−orbit interactions of RbCs and further analysis of the complex vibronic structures in region II are in progress.

Acknowledgment. This work was partially supported by MEST of Korea through the APRI-Research Program of GIST. We thank KRF for the financial support through ABRL (R14-2005-033-0100) and KOSEF for support through the Center for Intelligent NanoBio Materials (Grant R11-2005-008-00000-0). S.L. thanks KRF for financial support (KRF-2006-311-C00078) and KISTI supercomputing center (KSC-2007-S00-1028). The authors are grateful to Dr. Andrey V. Stolyarov for many helpful discussions.

Supporting Information Available: Data of the RbCs 640 nm system by RE2PI spectroscopy: (i) band constants of the $2\ ^3\Pi_0\ v' = 4-24 \leftarrow X\ ^1\Sigma^+\ v'' = 0$ transitions obtained by band-by-band fits and (ii) band constants of the $2\ ^3\Pi_1\ v' = 5$ and $3\ ^3\Sigma^+_1\ v' = 1 \leftarrow X\ ^1\Sigma^+\ v'' = 0$ transitions obtained by rotational band contour fits. This material is available free of charge via the Internet at http://pubs.acs.org.

Note Added after ASAP Publication. This article posted ASAP on July 17, 2008. Equation 1 has been revised. The correct version posted on July 31, 2008.

References and Notes

(1) DeMille, D. *Phys. Rev. Lett.* **2002**, *88*, 067901.
(2) Walter, J. M.; Barratt, S. *Proc. R. Soc. London, Ser. A* **1928**, *119*, 257.
(3) Loomis, F. W.; Kusch, P. *Phys. Rev.* **1934**, *46*, 292.
(4) Kusch, P. *Phys. Rev.* **1936**, *49*, 218.
(5) Katô, H.; Kobayashi, H. *J. Chem. Phys.* **1983**, *79*, 123.
(6) Gustavsson, T.; Amiot, C.; Vergès, J. *Chem. Phys. Lett.* **1988**, *143*, 101.
(7) Fellows, C. E.; Amiot, C.; Vergès, J. *J. Phys. II (France)* **1992**, *2*, 939.
(8) Fellows, C. E.; Gutterres, R. F.; Campos, A. P. C.; Vergès, J.; Amiot, C. *J. Mol. Spectrosc.* **1999**, *197*, 19.
(9) Gustavsson, T.; Amiot, C.; Vergès, J. *Mol. Phys.* **1988**, *64*, 293.
(10) Kim, B.; Yoshihara, K. *J. Chem. Phys.* **1994**, *100*, 1849.
(11) Kim, B.; Yoshihara, K. *Chem. Phys. Lett.* **1993**, *212*, 271.
(12) Yoon, Y.; Lee, Y.; Kim, T.; Ahn, J. S.; Jung, Y.; Lee, S. *J. Chem. Phys.* **2001**, *114*, 8926.
(13) Bergeman, T.; Fellows, C. E.; Gutterres, R. F.; Amiot, C. *Phys. Rev. A* **2003**, *67*, 050501(R).
(14) Bergeman, T.; Kerman, A. J.; Sage, J.; Sainis, S.; DeMille, D. *Eur. Phys. J. D* **2004**, *31*, 179.
(15) Pavolini, D.; Gustavsson, T.; Spiegelmann, F.; Daudey, J.-P. *J. Phys. B: At. Mol. Opt. Phys.* **1989**, *22*, 1721.
(16) Allouche, A. R.; Korek, M.; Fakherddin, K.; Chaalan, A.; Dagher, M.; Taher, F.; Aubert-Frécon, M. *J. Phys. B: At. Mol. Opt. Phys.* **2000**, *33*, 2307.
(17) Fahs, H.; Allouche, A. R.; Korek, M.; Aubert-Frécon, M. *J. Phys. B: At. Mol. Opt. Phys.* **2002**, *35*, 1501.
(18) Lim, I. S.; Lee, W. C.; Lee, Y. S.; Jeung, G.-H. *J. Chem. Phys.* **2006**, *124*, 234307.
(19) Lee, Y.; Yoon, Y.; Baek, S. J.; Joo, D.-L.; Ryu, J.; Kim, B. *J. Chem. Phys.* **2000**, *113*, 2116.
(20) Gerstenkorn, S.; Luc, P. *Atlas du Spectre d'Absorption de la Molécule d'Iode Entre 14800−20000 cm−1*; CNRS: Paris, 1978.
(21) Western, C. M. *PGOPHER version 5.2, a Program for Simulating Rotational Structure*; University of Bristol: U.K., 2007; http://pgopher.chm.bris.ac.uk.
(22) Mills, I.; Cvitaš, T.; Homann, K.; Kallay, N.; Kuchitsu, K. *Quantities, Units and Symbols in Physical Chemistry*; Blackwell: Oxford, U.K., 1993.
(23) Lefebvre-Brion, H.; Field, R. W. *The Spectra and Dynamics of Diatomic Molecules*; Elsevier: New York, 2004.
(24) Le Roy, R. J. *DParFit 3.3. A Computer Program for Fitting Multi-Isotopologue Diatomic Molecule Spectra*; University of Waterloo Chemical Physics Research ReportCP-660; University of Waterloo: Ontario, Canada, 2005.
(25) Herzberg, G. *Molecular Spectra and Molecular Structure I. Spectra of Diatomic Molecules*, 2nd ed.; Krieger: Malabar, India, 1989.
(26) Le Roy, R. J. *RKR1 2.0. A Computer Program for Implementing the First-Order RKR Method for Determining Diatomic Molecule Potential Energy curves;* University of Waterloo Chemical Physics Research ReportCP-657R; University of Waterloo: Ontario, Canada, 2004.
(27) Le Roy, R. J. *LEVEL 7.7. A Computer Program for Solving the Radial Schrödinger Equation for Bound and Quasibound Levels*; University of Waterloo Chemical Physics Research ReportCP-661; University of Waterloo: Ontario, Canada, 2005.

JP803360W